

Engineering Heritage Journal (GWK)

DOI: http://doi.org/10.26480/gwk.01.2024.51.59





ISSN: 2521-0904 (Print) ISSN: 2521-0440 (Online) CODEN: EHJNA9

RESEARCH ARTICLE

MULTI DETERMINISTIC BASED ASSESSMENT OF THE BEARING CAPACITY FOR A SHALLOW FOUNDATION: CASE STUDY OF LAGOS SOUTHWEST, NIGERIA

Oladipupo J.T.^a, Eze U. Stanley^b, Mohammad K. Ravari^c, S.H. Waziri^d, Saleh .A. Saleh^e, Orji M. Omafume^e, Avwenaghegha, J.O^f, Zainab Alaran^g

- a Research Hub, Geotech 4 all, Nigeria
- ^b Department of Applied Geology, Olusegun Agagu University of science and Technology Okitipupa Nigeria
- ^c International Institute of Numerical and Geo-foundation structure, Iran
- ^d Department of Geology, Federal University of Technology Minna, Nigeria
- ^e Department of Petroleum Engineering and Geoscience, Petroleum Training Institute, Effurun, Delta State, Nigeria
- Department of Physics, Delta State University of Science and Technology, Ozoro, Nigeria
- g Department of Applied Geology, Federal University of Technology Akure, Nigeria
- *Corresponding author email: uchechukwueze2014@gmail.com; dipupojeremiah@gmail.com

This is an open access article distributed under the Creative Commons Attribution License CC BY 4.0, which permits unrestricted use, distribution, and reproduction in any medium, provided the original work is properly cited.

ARTICLE DETAILS

Article History:

Received 17 November 2024 Revised 20 December 2024 Accepted 23 December 2024 Available online 16 January 2025

ABSTRACT

Shallow foundations are a popular and affordable foundation type for construction of buildings and engineering structures. Therefore, precise assessment of the underlying soil structure's bearing capacity is critical for their successful application. In this study, a multi-deterministic technique has been used to evaluate the bearing capacity of a shallow foundation. Empirical estimation of allowable bearing capacity (BC) was based on data from cone penetration tests employing the Schmertmann's approach. The BC generally increased with depth across all CPTs, aligning with the observed increase in cone resistance (qc) values. A strengthening soil profile was indicated by the overall rise in the average allowable bearing capacity with depth. The numerical modeling with Plaxis-3Dv24 software application accurately estimated the bearing capacity and settling behavior of the shallow foundation on lateritic clay. The findings are consistent with empirical estimates derived from CPT data, notably for allowable bearing capacity. The average bearing capacity estimated from CPT data was 604.98 KN/m², corresponding to an allowable bearing capacity of 201.66 KN/m². The numerical model predicted an ultimate bearing capacity of 620 KN/m², slightly higher than the empirical estimate, and resulting in an allowable bearing capacity of 206.67 KN/m² with a factor of safety (FoS) of 3 against shear failure. The calculated allowable bearing capacities from both methods are relatively close, indicating a reasonable level of agreement. In terms of settlement, the numerical model predicted initial settlement was 8.0 mm, well within the limiting settlement pressure, while for the empirical data settlement information was available for direct comparison. Therefore, the numerical model provided useful insights regarding settlement. It is critical to recognize that the numerical model's accuracy is strongly reliant on the input soil parameters (unit weight, Young's modulus, Poisson's ratio, cohesion, and friction angle), which were estimated based on field research data and engineering appraisal. Therefore, future research could use advanced constitutive models or laboratory testing to refine these values for more precise numerical simulations. The multi-deterministic technique can be extended to a broader range of case studies involving shallow foundations on lateritic clays, resulting in a more comprehensive database of design variables.

KEYWORDS

Applied load, Bearing capacity, Cone penetration test (CPT), Empirical estimation, Numerical modeling

1. Introduction

For a variety of constructions, shallow foundations are a popular and affordable foundation type (Tomlinson, 2013). A precise determination of the underlying soil structure's bearing capacity is necessary for their successful application (Briaud et al., 2010). The maximum load that a layer of soil can withstand without experiencing shear failure or endangering the foundation's structural integrity is referred to as bearing capacity (Das, 2018). Among other states, Lagos has seen a startling increase in building collapses and failures, with disastrous results for both people and property. On November 1, 2021, it was reported that a 21-story building on Gerard Road, Ikoyi, Lagos State, collapsed, killing numerous people (Premium Times Report, 2021). This was attributed to a number of

factors, including inadequate project management, a lack of quality assurance/control, and negligence on the part of the agencies in charge of the building project's approval and supervision (Das, 2018).

According to a Premium Times investigation, the Lagos State building moderators' egregious incompetence was evident in the building's density and obstruction on the property (Premium Times Report, 2021). Conventionally, in-situ testing techniques such as the Standard Penetration Test (SPT) or the Cone Penetration Test (CPT) are used to assess the bearing capability of shallow foundations (Fellenius, 2009). However, these methods have limitations, as they provide localized data and may not fully capture the complex stress-strain behavior of soil, particularly for heterogeneous formations like sandy lateritic clays (Hettiarachchi et al., 2016).

Quick Response Code	Access this article online				
	Website: www.gwk.com.my	DOI: 10.26480/gwk.01.2024.51.59			

Recent advancements in computational modeling have offered valuable tools for a more comprehensive evaluation of bearing capacity. Credit to the development of advanced numerical software application, like Plaxis-3Dv24, that allows engineers to simulate soil behavior under various loading conditions within a reasonable time, incorporating factors like soil strength parameters, drainage conditions, and foundation geometry (Whittle, 1993; Yu et al., 2011). The traditional methods typically rely on point-based data, providing insights only at specific locations. Numerical modeling extends this by offering three-dimensional visualizations of stress distribution, deformation, and failure mechanisms across the entire foundation area within reasonable time. This helps in better anticipating potential issues that might go unnoticed with simpler empirical methods (Griffiths and Fenton, 2000).

This study investigates the bearing capacity of a shallow foundation resting on firm to stiff sandy lateritic clay. It employs a combined field and numerical approach to achieve a more robust assessment. The field investigation program involves borehole exploration and Dutch Cone Penetration Tests (CPTs) to establish the soil properties and in-situ strength profile. The data obtained was further used within a numerical model developed using Plaxis-3Dv24 application to simulate the soil-foundation interaction and evaluate the bearing capacity. This study is aimed at characterizing the geotechnical properties of the firm to stiff sandy lateritic clay, evaluate the bearing capacity of the shallow foundation using standard CPT data and numerical modeling, and compare the results obtained from both approaches to assess their consistency and reliability.

1.1 Location of the study area, accessibility, topography and drainage

The research area is located in the northern portion of Lagos state, between latitude 6°30'57" and 6°30'57.600", and longitude 3°15'32" and 3°15'33". The site is accessible by Ikotun-Ijegun road, Isheri-Osun road, and other subsidiary routes, as illustrated in Figure 1. The landscape of the research region is undulating to flat, with elevations increasing only a few meters above sea level. During the wet season, the area is prone to flooding due to the rising water table. Natural drainage is generally supported by a network of dendritic streams. The study area's primary land use includes residential purposes, limited fishing and agricultural operations, local markets, and commercial companies. The region has a high population density and a well-established and dynamic community.

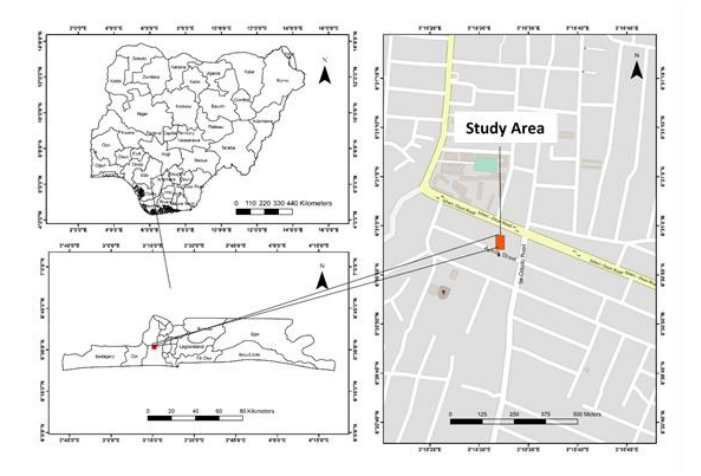


Figure 1: Location map of the study area

1.2 Local Geology of the Study Area

Lagos state, in southwestern Nigeria, is a confined marine environment with lagoons and sand barriers that restrict water flow, resulting in varied geomorphological zones along the coast. The Dahomey Plateau's lithological makeup is predominantly sand, clay, and limestone (Billman, 1992). As one moves westward, these lithologies strengthen and drop toward the shoreline. The Dahomey Plateau's stratigraphy has been split into six lithostratigraphic systems, ordered from oldest to youngest: Abeokuta, Ewekoro, Akinbo, Oshosun, Ilaro, and the Benin system (see Figure 2) (Okosun, 1990). Abeokuta is located within the basement complex and extends as a significant aquifer in the northern sector of Lagos State, particularly the Ikeja area, where well depths reach roughly 750.0 m.

In contrast, the llaro and Ewekoro formations in Lagos are mostly shale and clay and do not serve as aquifers. The only evidence on the hydraulic

features of the Ilaro Formation came from the Lakowe region, where no large aquifers were discovered. Identifying the Ewekoro Formation as an obvious aquifer within any rural well proved difficult. However, this system may have a restricted aquifer capacity in Lagos. The sandy layers along the shoreline form the greatest aquifer in Lagos, and they are linked by a network of wells. This formation is supported by a three-tiered structure of clay and silty layers, which contains several water reservoirs. The lagoon stretches from its entrance in the north to the southern coastal sections, with structural sands extending from the north.

Ijegun is located in the Benin Formation, which has a history spanning the Miocene to the present. The geology of Ijegun and its environs suggests the presence of aquifers in wetlands along the coastline, which penetrate the sediment at the lake's bottom. The sediments consist of unconsolidated, frequently coarse, compacted sands that transition into varying lateritic clays, as well as different plant deposits that contain partially carbonized minerals (peat). The surrounding landscape is generally composed of well-consolidated and dark brown clay layers that are more mature than the underlying brown clays, with a solid layer of pan material encountered between the current ground level and depths of up to 10.0 m within the excavated borehole.

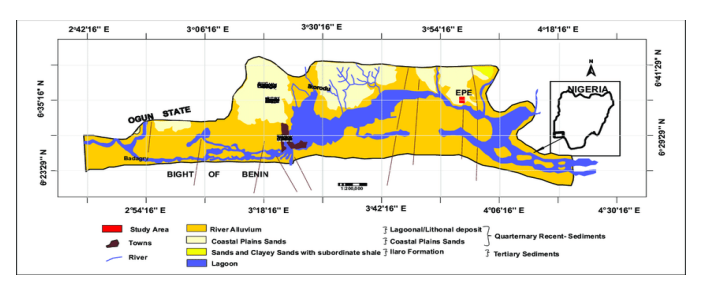


Figure 2: Geological Map of Lagos State, Nigeria, Showing the Study Area (adapted from Nigeria Geological Survey Agency, (NGSA, 2006)).

2. MATERIALS AND METHODS

2.1 Field Investigation

The field investigation program involved boring of one borehole (BH), and three Dutch Cone Penetration tests (CPT) were strategically executed at specific locations in the study area using the 2.50 tons machine to characterize the subsurface soil profile and obtain in-situ strength parameters. The borehole was drilled to a depth of 7.0 metres below the present ground surface, exhibiting subsoil conditions of stiff to very stiff sandy lateritic clay. The Cone Penetration Tests were carried out up to a refusal depth of 3.0 meters below the current ground level, with the cones anchoring due to the presence of stiff to very stiff sandy lateritic clay, which prohibited further penetration.

2.2 Laboratory Analysis

Laboratory analyses were performed on drill samples to offer detailed information on subsurface qualities. The following laboratory studies were performed on chosen samples in accordance with the British Standard (BS 1377: 2015) techniques of testing subsoil for civil engineering purposes.

2.2.1 Atterberg Limits Test

The consistency limit, also referred to as Atterberg's limit, is the water concentration at which soil shifts between two states (BS 1377-2015). The water content of the soil plays an important role in influencing the engineering properties of the subsurface. If the soil sample is sufficiently liquid, the liquid limit (LL) is the amount of water required to change the soil's condition from plastic to liquid. The plasticity limit (PL) is the amount of water at which a plastic changes to a semi-solid state (Jamal, 2020; Seed, 1967). The capacity of the liquid-plastic border to represent the kinds and concentrations of clay minerals found in fine fractions gives it practical significance.

High liquid limit and plasticity index values suggest that the soil has a high clay content and colloidal size of active minerals, as well as a poor bearing capacity (Skempton, 1953). The undisturbed soil samples collected during soil boring were used in this study. The samples were oven-dried to a consistent weight to assess their natural moisture content. For the liquid limit determination, a part of the soil sample was combined with distilled water to make a paste. The paste was placed in a regular cup, and a grooving tool was used to make a groove in the soil paste. The number of blows/drops required for the groove to shut was recorded, and the liquid limit was calculated using the moisture content.

To calculate the plastic limit, another fraction of the soil sample was

blended to create a plastic state soil. The soil was rolled into a thread of uniform diameter, the moisture content at which the thread broke was measured, and the plastic limit was calculated.

The plasticity index (Ip) was calculated as the difference between the liquid limit (LL) and the plastic limit (PL).

$$Ip=LL-PL$$
 (1)

2.2.2 Oedometer Consolidation Test

During the oedometer test, an undisturbed soil sample was collected at a depth of 1.50 m during soil boring. The sample was tailored to the dimensions of the oedometer cell. The sample was soaked after soaking in water for an appropriate amount of time. The saturated soil sample was inserted into the oedometer cell. A load increase was applied to the soil sample, and the resulting settlement was recorded. The coefficient of volume compressibility was determined by testing at various pressure ranges.

2.3 Empirical estimation of Subsoil Bearing Capacities

Using Schmertmann approach, the subsurface bearing capabilities were empirically estimated (Schmertmann, 1970). This technique was widely used to calculate a foundation soil's ultimate bearing capacity(qult) using cone resistance (qc) data from cone penetration tests (CPT). This technique offers a tried-and-true framework for converting data on cone penetration resistance into estimations of bearing capacity.

The Schmertmann's formula for calculating the ultimate bearing capacity is given as:

$$qult = (A * qc) + (C * \gamma' * Nc * Df)$$
 (2)

where:

qult = Ultimate bearing capacity (in force per unit area, typically in kPa)

qc = Cone resistance (in force per unit area, typically in MPa)

A = Area ratio factor

C = Pore pressure coefficient

 γ' = Effective unit weight of the soil (in force per unit volume, typically in $kN/m^3)$

Nc = Cone factor

Df = Depth factor

2.4 Numerical modeling of Subsoil Bearing Capacities

Based on the CPT analysis at depth of 1.25 meters a surface load of 817.93 KN/m 2 was applied and was used for the numerical modeling, together with the input soil parameters shown in Table 1 that was obtained from laboratory analysis of retrieved soil samples from the borehole.

Table 1: Input soil parameters for Numerical modeling							
Parameter	Name	Clay	Unit				
General							
Material Model	Model	Mohr-Coulomb	-				
Drainage type	Туре	Drained	-				
Soil Unit weight above P.I	γ_{unsat}	16	KN/m³				
Soil Unit weight below P.I	γ_{sat}	18	KN/m³				
Shear Strength							
Young modulus	E'	340000	KN/m³				
Poisson's ratio	ν'	0.35					
Cohesion	C'ref	68	KN/m³				
Friction angle	φ'	13	-				
Dilatancy angle	Ψ	0	-				

The Plaxis-3Dv24 application program was used to carry out the numerical modeling. The development of the model took place in four phases. Initially, the program was used to generate a virtual depiction of the soil stratigraphy using the drill data and input soil parameters obtained in the laboratory (Table 1). Secondly, the model was fitted with a surface load equal to the ultimate carrying capacity (-817.93 $\rm KN/m^2)$ as determined by CPT. Next was the model geometry which was discretized

using the Jenkins approach during the mesh production phase. From the soil model realized the software program generated nodes mathematically connected using the finite element modeling (FEM) procedure.

In order to focus the stress effects on the vital zone, this approach permits mesh refinement around the foundation region while ensuring effective mesh dispersion. Ultimately, there were two stages of calculation in the modeling process. In Phase 1, the surface load was deactivated and the model's starting stress conditions were established. After reactivating the surface load, Phase 2 computed the soil mass deformations and stress distribution that resulted. This two-phase method made it easier to comprehend how the foundation load caused changes in stress, which made it possible to estimate bearing capacity using a numerical method in the future. It is crucial to recognize that the input parameters in Table 1 have a significant impact on the correctness of the numerical model. Based on the data from the field study and engineering judgment, the Mohr-Coulomb model with drained conditions and the selected soil properties (unit weight, Young's modulus, Poisson's ratio, cohesion, and friction angle) were assumed.

3. RESULTS AND ANALYSIS

3.1 Soil Profile, Borehole log section and Laboratory test results

The subsoil lithologies observed at different depth within the borehole is shown in Table 2, while the borehole section is presented in Figure 3. The results of cone penetration test (CPT), atterberg limits, undrained triaxial and Oedometer consolidation tests are summarized in Tables 3, 4, and 5. The variation of CPT with respect to depth is shown in Figure 4, while the graphs of undrained triaxial and consolidation tests are shown in Figures 5 and 6 respectively.

Table 2: Summary of Subsoil lithologies encountered at different depth within the borehole

Depth Range (m)

0.0 to 0.75

Firm, reddish brown, silty, sandy, lateritic CLAY

0.75 to 2.25

Firm becoming stiff, reddish brown, silty sandy lateritic CLAY

2.25 to 7.0

Stiff becoming very stiff, reddish brown, silty, sandy lateritic CLAY with fine to coarse gravel.

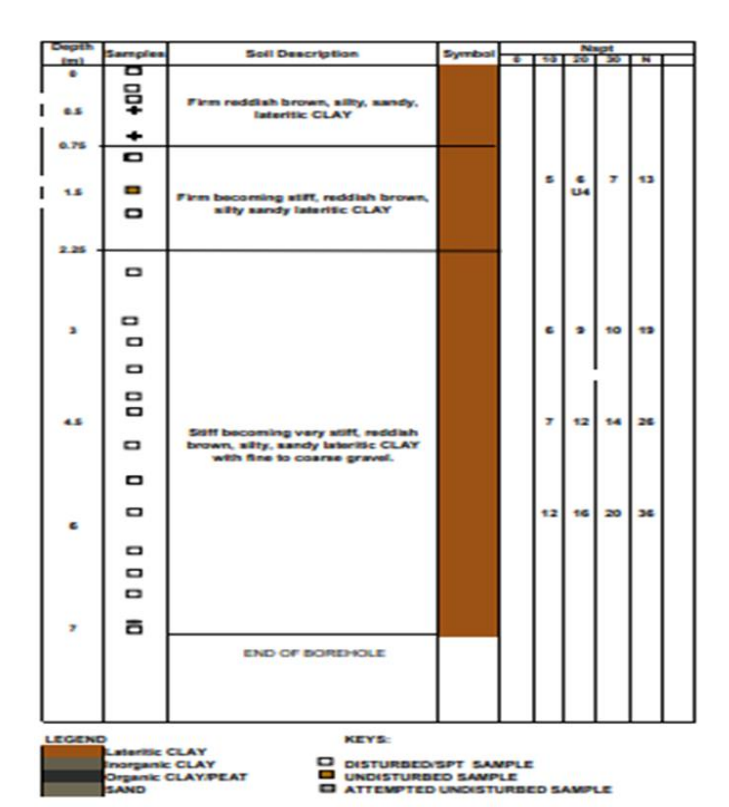


Figure 3: Borehole log section

Table 3: Summary of cone penetration test (CPT) result					
Depth (m)	CPT 1	CPT 2	СРТ 3		
Depth (III)	Qc	Qc	Qc		
0.25	20	20	15		
0.5	15	25	20		
0.75	20	30	40		
1	25	40	40		
1.25	10	50	50		
1.5	20	70	60		
1.75	30	70	70		
2	40	75	70		
2.25	50	80	75		
2.5	70	92	75		
2.75	90	11	110		
3	115	11	120		

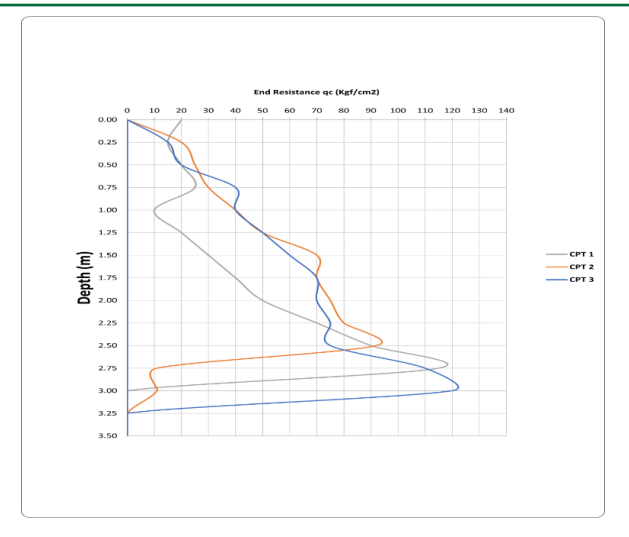


Figure 4: Chart of Cone resistance (qc) for CPT-1, 2, and 3 versus Depth (m)

Table 4: Atterberg Limits Results					
Natural Moisture Content (M.C)	A	tterberg Limi	gB		
	LL	PL	PI		
	%	%	%		
%	Dw	Dw	dw	Mg/m³	
19	40	23	17	1.87	
18	38	19	19		
21	40	22	18		

	Table 5: Result of Undrained triaxial and Oedometer consolidation tests							
Quick Undrained Triaxial Tests			Lab.	Oodomote	Oedometer Consolidation			
	Quick Onuramed	u IIIaxiai Tests		Vane	— Oedometer Consolidation			
Dia.	S ₃	Cu	Ø	Su	Stress	$M_{\rm v}$	C_{v}	
Туре	- I/NI / 2	L/N / 2	Dec	IZNI / 2	Dance VN /m²	2 /MNI	2 /	
(mm)	KN/m ²	KN/m ²	Deg.	KN/m²	Range KN/m ²	m ² /MN	m²/yr	
38	100	68	13		50 - 100	0.133	2.2	
	200				100 - 200	0.247	2.6	
	400				200 - 400	0.152	2.5	
					400 - 800	0.105	2.3	

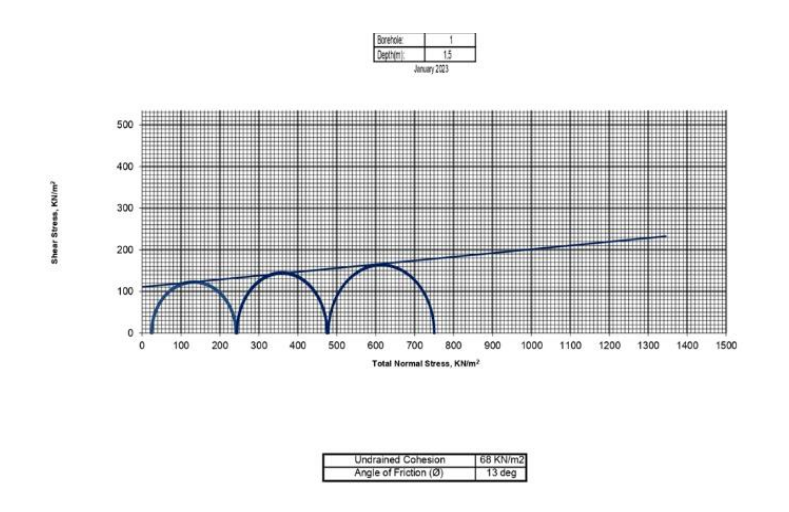


Figure 5: Undrained triaxial test graph

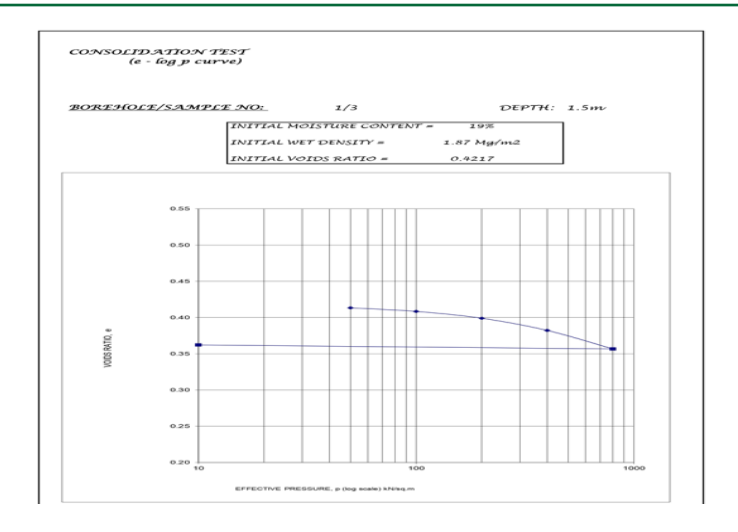


Figure 6: Consolidation test graph

3.2 Empirically derived Ultimate bearing capacity and allowable bearing capacity results from cone penetration test (CPT)

Based on the results to the three (3) cone resistance tests conducted the

ultimate bearing capacity (UBC), and the allowable bearing capacity (ABC) estimated empirically are shown in Tables 6, 7, and 8. Figure 7 is a chart of average allowable bearing capacity against depth (m).

Table 6: Computed Ultimate Bearing Capacity and Allowable Bearing Capacity from Cone Resistance (CPT-1)					
Depth (m)	Cone Resistance	Undrained Shear Strength	Ultimate Bearing Capacity	Allowable Bearing	
	(kgf/cm ²)	(KN/m²)	(KN/m²)	Capacity (KN/m²)	
0.00		0.00	0.00	0.00	
0.25	20	111.82	323.30	107.77	
0.50	15	83.53	247.31	82.44	
0.75	20	111.29	331.04	110.35	
1.00	25	139.04	414.77	138.26	
1.25	10	54.72	179.07	59.69	
1.50	20	110.49	342.66	114.22	
1.75	30	166.27	506.24	168.75	
2.00	40	222.05	669.83	223.28	
2.25	50	277.82	833.42	277.81	
2.50	70	389.64	1156.72	385.57	
2.75	90	501.45	1480.02	493.34	
3.00	115	641.29	1883.17	627.72	

Table 7: Computed Ultimate Bearing Capacity and Allowable Bearing Capacity from Cone Resistance (CPT-2)					
Depth (m)	Cone Resistance (kgf/cm²)	Undrained Shear Strength (KN/m²)	Ultimate Bearing Capacity (KN/m²)	Allowable Bearing Capacity (KN/m²)	
0.00	-	0.00	0.00	0.00	
0.25	20	111.82	323.30	107.77	
0.50	25	139.57	407.03	135.68	
0.75	30	167.33	490.76	163.59	
1.00	40	223.10	654.34	218.11	
1.25	50	278.88	817.93	272.64	
1.50	70	390.69	1141.23	380.41	
1.75	70	390.43	1145.10	381.70	
2.00	75	418.19	1228.83	409.61	
2.25	80	445.94	1312.56	437.52	
2.50	92	512.93	1508.09	502.70	
2.75	115	641.55	1879.30	626.43	
0.00	-	0.00	0.00	0.00	

	Table 8: Computed Ultimate Bearing Capacity and Allowable Bearing Capacity from Cone Resistance (CPT-3)					
Depth (m)	Cone Resistance (kgf/cm²)	Undrained Shear Strength (KN/m²)	Ultimate Bearing Capacity (KN/m²)	Allowable Bearing Capacity (KN/m²)		
0.00	0.00	0.00	0.00	0.00		
0.25	15	83.80	243.44	81.15		
0.50	20	111.55	327.17	109.06		
0.75	40	223.37	650.47	216.82		
1.00	40	223.10	654.34	218.11		
1.25	50	278.88	817.93	272.64		
1.50	60	334.65	981.51	327.17		
1.75	70	390.43	1145.10	381.70		
2.00	70	390.17	1148.97	382.99		
2.25	75	417.92	1232.70	410.90		
2.50	75	417.66	1236.57	412.19		
2.75	110	613.53	1799.44	599.81		
3.00	120	669.31	1963.03	654.34		

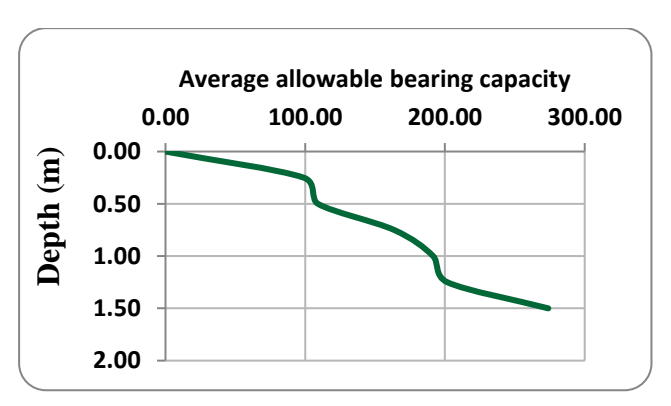


Figure 7: Graph of average allowable bearing capacity against depth (m)

3.3 Numerical solution results

Based on the numerical analysis procedure the results of the soil model, deformed mesh and total displacement resulting from the applied load are presented in Figures 8, 9, 10, and 11. The numerical calculations and derived bearing capacity at maximum load are summarized in Tables 9 and 10. Figure 11 is the curve of applied load against the soil displacement derived from the numerical solution using the Plaxis-3Dv24 application.

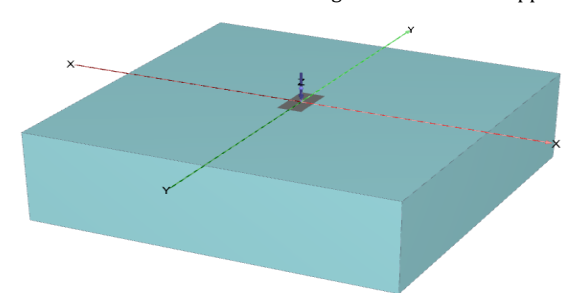


Figure 8: 3D soil model

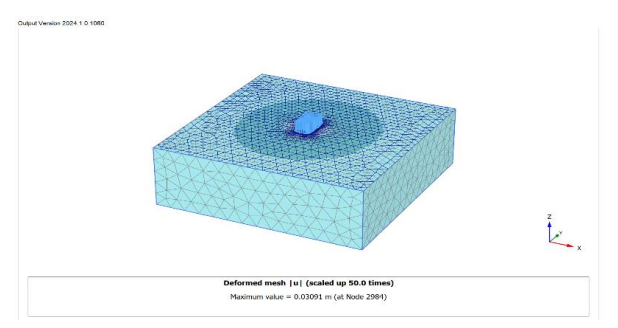


Figure 9: Generated deformed mesh

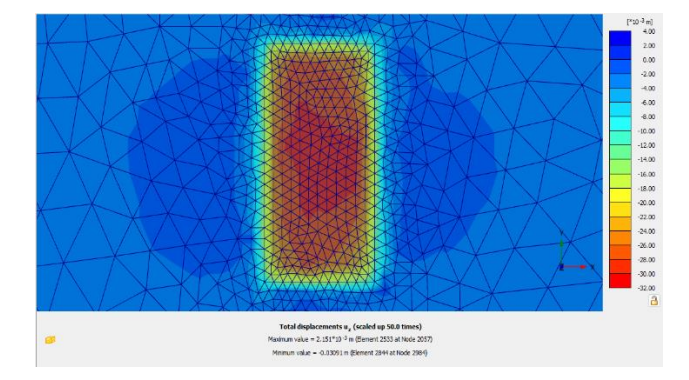


Figure 10: Generated Total displacement (uz) result (Top View)

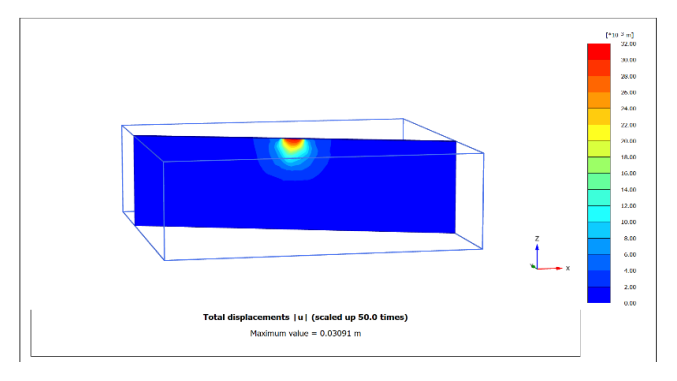


Figure 11: Vertical cross-sectional view of generated Total displacement result $I_{U}I$

	Table 9: Summary of Numerical calculation at maximum load applied						
Point	Phase	Step	u_z [m]	ΣM Stage	Soil Displacement (mm)	Applied Load (KN/m²)	
0	0	0	N/A	0.00E+00			
1	1	1	0.00E+00	0.00E+00	0	0.00E+00	
2	1	1	-2.43E-03	2.18E-01	2.433574	1.78E+02	
3	1	2	-4.88E-03	4.24E-01	4.879849	3.47E+02	
4	1	3	-6.14E-03	4.96E-01	6.143581	4.05E+02	
5	1	4	-7.42E-03	5.55E-01	7.422452	4.54E+02	
6	1	5	-8.71E-03	6.07E-01	8.711562	4.96E+02	
7	1	6	-1.00E-02	6.51E-01	10.00854	5.33E+02	
8	1	7	-1.13E-02	6.91E-01	11.3104	5.65E+02	
9	1	8	-1.26E-02	7.27E-01	12.61749	5.95E+02	
10	1	9	-1.53E-02	7.90E-01	15.25108	6.46E+02	
11	1	10	-1.79E-02	8.42E-01	17.90912	6.88E+02	
12	1	11	-2.06E-02	8.85E-01	20.57989	7.24E+02	
13	1	12	-2.33E-02	9.23E-01	23.26117	7.55E+02	
14	1	13	-2.60E-02	9.56E-01	25.95091	7.82E+02	
15	1	14	-2.73E-02	9.70E-01	27.29816	7.93E+02	
16	1	15	-3.00E-02	9.94E-01	29.9853	8.13E+02	
17	1	16	-3.07E-02	1.00E+00	30.74001	8.18E+02	

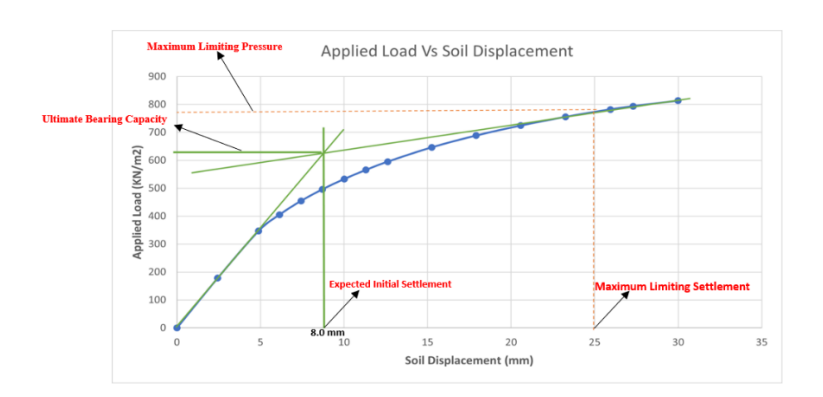


Figure 12: Graph of Applied load versus Soil displacement derived from numerical analysis using Plaxis-3Dv24

Table 10: Summary of Numerically derived bearing capacities					
Numerical Estimations	Value	Unit			
Ultimate Bearing Capacity (qult)	620	KN/m ²			
Factor of Safety against shear failure	3				
Allowable Bearing Capacity against shear failure (qa)	206.67	KN/m²			
Limiting Settlement for foundation	25	Mm			
Corresponding Limitting Pressure	780	KN/m²			
Design Bearing Capacity	206.67	KN/m ²			
Expected Initial Settlement	8	Mm			

3.4 Discussion of Results

The study's findings indicate that three separate soil layers were found in the borehole and were distinguished by their color, consistency, and particle size. The predominant subsurface lithology in the research area is lateritic soil, which can range from firm to stiff lateritic clay (Table 2). The change from firm to very stiff clay was a sign that the strength of the soil increased with depth. Between 2.25 and 7.0 meters, a gravel layer was found, indicating a perhaps stronger soil profile (Table 2). A denser and maybe stronger soil profile with depth is suggested by the slow increase in stiffness and the presence of gravel in the lower layers. The drilling log's full information is shown in Figure 3.

The cone penetration test results show that cone penetration resistance (qc) values increased with depth, indicating a trend of increasing soil strength (Table 3). At shallow depths (0.25m to 1.25m) showed some variability in qc values, potentially due to near-surface inconsistencies (Figure 4). Deeper depths (beyond 1.25m) exhibited a more pronounced increase in qc values, reaching up to 115 to 120 MPa (Table 3). This significant increase in strength suggests denser soil packing with significant strength gains or the presence of the gravel layer observed in the borehole data between 2.25 and 3.0 m (Figure 4).

In the study of subsurface features, the atterberg limits results give useful information on the physical properties of the cohesive subsoil under investigation. The results of atterberg limits tests on subsurface samples recovered from the borehole at depths of 1.50 m, 3.00 m, and 6.75 m revealed that the subsoil is composed of lateritic clay with firm to stiff/very stiff consistency and a medium to low plasticity index. Table 4 shows that the soil samples had natural moisture content (NMC) values of 19%, 18%, and 21%. The NMC represents the percentage of water content in the soil in its natural form. These data place the soil in the A-6 group according to the AASHO soil categorization system. The Liquid Limit (LL) values range between 38% and 40%, with an average of 39.33% (Table 4). These numbers represent the moisture content at which the soil transforms from plastic to liquid state. The Plastic Limit (PL) values range from 19% to 23%, with an average of 21.33% (see Table 4). PL denotes the moisture content at which the soil fails to behave plastically. The Plasticity Index (PI) ranges from 17.0 to 19.0%, with an average of 18.33% (Table 4). PI is a measure of the soil's plasticity and an important component in soil categorization. The dry weight density of the soil represented as (gB) has a value of 1.87 Mg/m³ (Table 4).

These measurements indicate the compactness and weight of the soil,

which are critical considerations in engineering design and construction. In conclusion, the Atterberg Limits data collectively indicate that the cohesive subsoil has moderate to high flexibility, as demonstrated by the relatively limited range of the flexibility Index. The moisture content, plasticity, and density data all contribute to a thorough understanding of the soil's behavior, assisting in the assessment of its suitability for certain engineering applications and informing foundation design and construction decisions.

The undrained triaxial test and Oedometer consolidation results provide critical information about the mechanical properties and compressibility characteristics of the subsoil under investigation. The fast undrained triaxial test varied the applied stress from 50 to 800 kN/m², resulting in an increase in the undrained shear strength (Su) from 0.133 kN/m² to $0.105 \ kN/m²$ (see Table 5). This represents the soil's ability to withstand shear deformation under undrained conditions. The Vane Shear Test with a 38 mm vane diameter yielded a cohesive unit (Cu) of 68 kN/m² (Table 5), showing soil shear strength.

Oedometer consolidation experiments were performed at stress levels ranging from 100 to 800 kN/m² (see Table 5). Table 5 shows that the coefficient of volume compressibility (Mv) decreased from 0.133 m²/MN to 0.105 m²/MN as applied stress increased. This pattern implies that the subsurface is composed of sandy lateritic clay of low to medium compressibility. The coefficient of consolidation (Cv) indicated the soil's consolidation rate under stress, ranging from 2.2 to 2.6 m²/yr (Table 5).

In general, the results indicate that the subsurface has high undrained shear strength, indicating that it can tolerate shear deformation. The Oedometer consolidation results support this by emphasizing the soil's compressibility properties, which indicate sandy lateritic clay with moderate consolidation rates. By defining the engineering characteristics of the soil, these results are essential for well-informed geotechnical evaluations that aid in the planning and implementation of building projects. Referring to Figures 5 and 6 are the undrained triaxial test and consolidation graphs.

Empirical estimation of allowable bearing capacity (BC) was based on qc values employing the Schmertmann's approach (Tables 6, 7, and 8). The BC generally increased with depth across all CPTs, aligning with the observed increase in qc values. Between CPTs, differences in BC were noted, indicating possible geographical heterogeneity in the soil. In comparison to CPT-2 and CPT-3, CPT-1 displayed a lower BC at 1.25 m. A strengthening soil profile was indicated by the overall rise in the average allowable bearing capacity with depth (Figure 7).

The numerical modeling with Plaxis-3Dv24 yielded valuable insights into the soil-foundation interaction and bearing capacity of the shallow foundation on lateritic clay. With a factor of safety (FoS) of 3 against shear failure, the model anticipated an ultimate bearing capacity (qult) of 620 KN/m², which translates to an allowed bearing capacity (qa) of 206.67 kN/m², as seen in Table 10. For shallow foundations, this safety factor is in line with standard design guidelines (Tomlinson, 1994).

The resulting deformed mesh (Figure 9) and total displacement data (Figures 10 and 11) show soil deformation patterns as load increases. The greatest expected initial settlement was 8.0 mm, which falls within the limiting settlement of 25.0 mm for a limiting pressure of 780 kN/m² (Table 10), as stipulated by British Standards (BS 8102-1:2013). This shows satisfactory foundation performance with little settlement under the specified load. The load-displacement graph (Figure 12) supports this discovery by showing a somewhat linear relationship at the design load, followed by a steeper increase at higher loads, indicating the commencement of possible failure.

These results are consistent with previous research on Nigerian lateritic soils. For example, a group researchers, looked at the carrying capability of shallow foundations on cohesive tropical soils in southwestern Nigeria (Alawode et al., 2020). The study found that bearing capabilities can range from 180 to 250 kN/m², depending on soil profile. This study's estimated bearing capacity of 206.67 kN/m² is within this range, demonstrating the validity of the numerical modeling approach and its relevance to lateritic clays in Nigeria.

4. CONCLUSION

A multi-deterministic technique has been used to analyze the bearing capability of a shallow foundation. The numerical modeling with Plaxis-3Dv24 software application accurately anticipated the bearing capacity and settling behavior of the shallow foundation on lateritic clay. The findings are congruent with empirical estimates derived from CPT data, notably for allowable bearing capacity. The average bearing capacity estimated from CPT data was 604.98 KN/m², corresponding to an

allowable bearing capacity of 201.66 $\rm KN/m^2$. The numerical model predicted an ultimate bearing capacity of 620 $\rm KN/m^2$, slightly higher than the empirical estimate, and resulting in an allowable bearing capacity of 206.67 $\rm KN/m^2$. The calculated allowable bearing capacities from both methods are relatively close, indicating a reasonable level of agreement.

In terms of settlement, the numerical model predicted initial settlement was 8.0 mm, well within the limiting settlement pressure, while for the empirical data on settlement information was available for direct comparison. Therefore, the numerical model provided useful insights regarding settlement that could not be estimated directly from field data. It is critical to recognize that the numerical model's accuracy is strongly reliant on the input soil parameters (unit weight, Young's modulus, Poisson's ratio, cohesion, and friction angle), which were estimated based on field research data and engineering judgment. Future research could use advanced constitutive models or laboratory testing to refine these values for more precise numerical simulations.

Based on these results, we recommend that additional field studies, such as plate load testing, can be used to directly evaluate the numerical model's predictions and improve the input parameters. Further research can look at the use of more advanced constitutive models to describe the complex behavior of lateritic clays, particularly under cyclic loading circumstances. In addition, sensitivity analysis should be performed to determine the effect of changes in input parameters on estimated bearing capacity and settlement. Finally, the multi-deterministic technique can be extended to a broader range of case studies involving shallow foundations on lateritic clays, resulting in a more comprehensive database of design variables.

ACKNOWLEDGEMENT

We are incredibly grateful to International institute of Numerical and Geofoundation structure, for the use of her computing facilities and to the Federal University of Technology Minna, Nigeria for the use of her laboratory platform.

FUNDING

There was no grant or financial support provided from any agency in the public, commercial, and not-for profit organization for this research work

AVAILABILITY OF DATA

Applicable and available on demand from the corresponding author

DECLARATIONS

Ethical Approval Not applicable.

Conflicts of interest/Competing interests

We declare that this research work has never been submitted previously by anyone to any journal for peer review and publication, hence it is an original work. All the ethical principles of research were implemented.

REFERENCES

- Alawode, O.O., Adedokun, A.A., Ijimoore I.A., 2020. Assessment of bearing capacity of soils for foundation design using Plaxis 3D. Int J Civ Eng Technol., 11 (12), Pp. 1828-42.
- Billman H.G., 1992. Offshore stratigraphy and paleontology of the Dahomey Embayment, West Africa. Nig. Assoc Pet Explor., 7, Pp. 121-30.
- Briaud, J.L., Ballas, J.N., Garnier, J.P., 2010. A framework for design verification of shallow foundations. J Geotech Geoenviron Eng., 136 (5), Pp. 653-63. Available from: https://www.researchgate.net/publication/272492627_Design_of_shallow_foundations_based_on_design_method
- British Standard. BS 1377:2015. Methods of test for soils for civil engineering purposes. Milton Keynes: British Standards Institution.
- BSI. BS 8102-1:2013-Code of practice for performance of building structures. London: British Standards Institution
- Das, B.M., 2018. Principles of foundation engineering. 8th ed. Cengage Learning.
- Fellenius, B.H., 2009. Settlement calculations of engineering structures. CRC Press.
- Griffiths D., Fenton G., 2000. Influence of soil strength spatial variability on the stability of an undrained clay slope by finite elements.

- Geotech Spec Publ., Pp. 184-93. doi:10.1061/40512(289)14.
- Hettiarachchi, K.R., Karunarathne, N.P., Nawaratne, N.S., 2016. Analysis of shallow foundation on Sri Lankan residual soils using finite element method. Int J Geotech Eng., 10 (2), Pp. 182-93. Available from: https://istasazeh-co.com/wp-content/uploads/2022/07/Shallow-Foundations-Discussions-and-Problem- Solving-Tharwat-M-Baban.pdf
- Jamal, H., 2000. Atterberg limits soil classification: liquid limit, plastic limit, shrinkage. About Civil [Internet]. 2020 [cited 2023 Dec 26]. Available from: www.aboutcivil.org
- Nigeria Geological Survey Agency (NGSA). 2006. Geological Map of Lagos State, Nigeria, showing the study area. Available at www.Nig. Geo. Survey agency (NGSA)
- Okosun, E.A., 1990. A review of the Cretaceous stratigraphy of the Dahomey Embayment, West Africa. Cretaceous Res., 11, Pp. 17-27.
- Premium Times. Ikoyi building collapse. Premium Times [Internet]. 2021. [citeDs, d 2023 Oct 30]. Available from: https://www.premiumtimesng.com/news/505583-ikoyibuilding-collapse

- Schmertmann, J.H., 1970. Static cone to compute static settlement over sand. J. Soil Mech Found Div ASCE., 96 (3), Pp. 1011-43. Available from: https://ascelibrary.org/doi/10.1061/JSFEAQ.0001418
- Seed H.B., Woodward R.J., Lundgren R., 1967. Fundamental aspects of the Atterberg limits. J Soil Mech Found Div., 92 (SM4), Pp. 63-4.
- Skempton, A.W., 1953. The colloidal activity of clay. Proc Int Conf Soil Mech Found Eng., 1, Pp. 57-61.
- Tomlinson, M.J., 1994. Pile design and construction practice. CRC Press.
- Tomlinson, M.J., 2014. Pile design and construction practice. CRC Press; 2014. Available from: https://menglim498.files.wordpress.com/2013/04/pile-design-and-construction.pdf
- Whittle, A.J., 1993. Settlement and bearing capacity of foundations on cohesive soil. Ground Eng., 26 (8), Pp. 25-30. Available from: https://www.icevirtuallibrary.com/doi/10.1680/gasi.31708.fm
- Yu, H., Sha, F., Wang, J., 2011. Three-dimensional numerical modeling of foundation bearing capacity on layered soil. Comput Geotech., 38 (1), Pp. 1-10. Available from: https://link.springer.com/article/10.1007/s40891-023-00461-y

